UNIFORM SCALAR QUANTIZATION BASED WYNER-ZIV CODING OF LAPLACE-MARKOV SOURCE

Vadim Sheinin, Ashish Jagmohan, Dake He

IBM T. J. Watson Research
Email: vadims@us.ibm.com, ashishja@us.ibm.com, dakehe@us.ibm.com

ABSTRACT

Wyner-Ziv coding has recently emerged as an alternative to conventional DPCM coding for compression of sources with memory, particularly in video compression. This paper studies the operational rate-distortion performance of Wyner-Ziv coding, using uniform scalar quantization followed by perfect Slepian-Wolf coding, for compression of a Laplace-Markov source. The performance gap of this technique relative to DPCM coding is characterized through derived rate-distortion expressions and numerical simulations.

***Index Terms*—** Quantization, source coding, Wyner-Ziv coding, differential pulse code modulation, Laplace-Markov source

1. INTRODUCTION

Differential Pulse Code Modulation (DPCM) is a well-known source coding technique used for compression of sources with memory. It is based on the simple idea of using previously encoded symbols as side-information available at both encoder and decoder. This side-information is used to differentially encode the current-source symbol. In practical applications DPCM is often used in conjunction with scalar quantization, which provides good compression efficiency at low computational cost.

Consider a discrete-time stationary source $\{X_n\}_{n\in\mathbb{Z}}$ with joint densities $f_{X_1,\ldots,X_n}(x_1,\ldots,x_n)$ for $n \in \mathbb{Z}$. An infinite-level scalar quantizer is defined by a countably infinite set of thresholds $\mathcal{T} = \{t_i\}_{i\in\mathbb{Z}}$, a countably infinite set of reconstruction levels $\mathcal{R} = \{y_i\}_{i\in\mathbb{Z}}$, an integer-valued quantization function $Q(x) = i \ \ \forall x \in [t_i, t_{i+1}]$ and a real-valued reconstruction function $R(x) = y_i \ \ \forall x \in [x_i, x_{i+1}]$. A uniform scalar quantizer is an infinite-level scalar quantizer with $t_i - t_{i-1} = \Delta$ for a constant $\Delta > 0$, for all $i \in \mathbb{Z}$. Denoting the decoder reconstruction of symbol X_n as $\widehat{X}_n$, a typical DPCM encoder communicates to the decoder[1]

$$\tau_n \triangleq Q(X_n - E[X_n|\widehat{X}_{n-1},\ldots,\widehat{X}_{n-h}]) \tag{1}$$

where $E[\cdot]$ denotes the expectation operator, and $\{\widehat{X}_{n-1},\ldots,\widehat{X}_{n-h}\}$ is the side-information. The corresponding DPCM decoder reconstructs symbol X_n as

$$\widehat{X}_n = E[X_n|\tau_n,\widehat{X}_{n-1},\ldots,\widehat{X}_{n-h}] \tag{2}$$

Assuming perfect entropy coding, the performance of DPCM can be characterized by the following rate and mean-squared distortion

$$R_{DPCM} = \lim_{N\to\infty}\frac{1}{N}\sum_{n=1}^{N} H(\tau_n)$$

$$D_{DPCM} = \lim_{N\to\infty}\frac{1}{N}\sum_{n=1}^{N} E[(X_n-\widehat{X}_n)^2]$$

[1]We assume the commonly used mean-squared error metric as the metric of interest, throughout this paper.

where $H(\cdot)$ is the entropy function.

A popular (and for us, motivating) application of DPCM is video coding—current video-coding standards such as MPEG-* typically employ DPCM coding which uses uniform-scalar quantizers with dead-zones, one or two previous video frames as side-information, and with $E[\cdot]$ in (1) approximated using motion estimation.

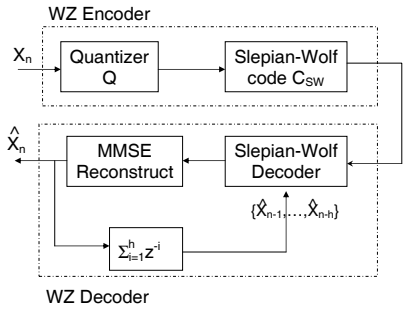

Fig. 1. WZ compression for source with memory.

In recent years there has been much interest in the use of Wyner-Ziv (WZ) coding as an alternative to DPCM in video compression applications. WZ coding [1] is lossy source coding with side-information assumed present solely at the decoder. Figure 1 shows a typical WZ coding system for compression of a source with memory. The WZ encoder communicates, at time n,

$$\tau_n^{WZ} \triangleq C_{SW}(Q(X_n)) \tag{3}$$

where C_{SW} denotes a Slepian-Wolf (SW) code [2, 3]. The decoder decodes $Q(X_n)$ using τ_n^{WZ} and the side-information $\{\widehat{X}_{n-i}\}_{i=1}^{h}$, and then reconstructs the source symbol as

$$\widehat{X}_n = E[X_n|Q(X_n),\widehat{X}_{n-1},\ldots,\widehat{X}_{n-h}]$$

Assuming perfect SW coding, the performance of WZ coding can be characterized by the rate given by the Slepian-Wolf theorem [2]

$$R_{WZ} = \lim_{N\to\infty}\frac{1}{N}\sum_{n=1}^{N} H(Q(X_n)|\widehat{X}_{n-1},\ldots,\widehat{X}_{n-h}) \tag{4}$$

and the distortion

$$D_{WZ} = \lim_{N\to\infty}\frac{1}{N}\sum_{n=1}^{N} E[(X_n-\widehat{X}_n)^2] \tag{5}$$

The use of WZ coding in video compression is motivated by the observation that $C_{SW}(Q(X_n))$ in (3) is, typically, significantly less costly to compute as compared to $E[\cdot]$ in (1). Thus, WZ coding can facilitate low-complexity encoding [4], which is desirable in many applications.

While the performance of Wyner-Ziv coding using scalar quantization has been analyzed previously for memoryless sources [5], an open question is the performance loss of the above WZ system compared to the conventional DPCM system.

The main objective of the present paper is to analyze the compression performance of uniform scalar quantization based WZ coding for compression of a source with memory. Motivated by video coding, we are specifically concerned with the stationary, first-order Laplace-Markov source which is well-known to be a good source model for video (cf. [6, 7]). The source can be described as

$$X_n = rX_{n-1} + Z_n \tag{6}$$

where the marginal density of X_n is $f_X(x) = \frac{\lambda}{2}e^{-\lambda|x|}$, r is the real-valued correlation coefficient, and $\{Z_n\}$ is an i.i.d. zero-mean, innovation sequence with Z_n independent of X_{n-1}. As has been shown by [8], the marginal density of Z_n is given by a weighted sum of the density of X_n and an impulse density

$$f_Z(z) = r^2\delta(z) + (1-r^2)\frac{\lambda}{2}e^{-\lambda|z|} \tag{7}$$

In Section 2, we analyze the rate-distortion performance of WZ coding, using uniform scalar quantization and perfect SW coding, for a memoryless source-side information pair with channel noise with marginal distribution $f_z(z)$. In Section 3 we extend our analysis to the case where the source has memory—in particular we consider compression of the Laplace-Markov source in (6) using WZ coding, where the decoder uses $Q(X_{n-1})$ as side-information. In Section 4 we compare the rate-distortion performance of WZ coding using uniform scalar quantization to that of DPCM coding in order to characterize the performance gap between the two techniques.

2. WZ CODING OF MEMORYLESS SOURCE USING UNIFORM SCALAR QUANTIZATION

We consider the asymmetric uniform scalar quantizer with partition levels $\{t_k = -\frac{\Delta}{2}+k\Delta\}_{k\in\mathbb{Z}}$, where Δ is the quantization interval. Let X, Y be memoryless, stationary zero-mean Laplacian sources such that $X = rY + Z$ where Z is independent of Y and has density $f_Z(z)$ given by (7), $f_X(x) = \frac{\lambda}{2}e^{-\lambda|x|}$ and $f_Y(y) = \frac{\lambda}{2}e^{-\lambda|y|}$. Our aim, in this section, is to compute the operational rate-distortion performance of WZ coding, using the quantizer described above and perfect SW coding, for the source X given the decoder side-information Y.

To this end, we begin by considering the operational rate-distortion function for uniform scalar quantization of the random variable $\widehat{Z}$ with density $f_{\widehat{Z},\epsilon}(z) = f_z(z-\epsilon\Delta)$ where f_z is as given in (7), and $-\frac{1}{2} \le \epsilon < \frac{1}{2}$. We define $p_k \triangleq \int_{t_k}^{t_{k+1}} f_X(x)dx$, and denote the rate and distortion by R_ϵ and D_ϵ respectively. Then $R_\epsilon = -\sum_{k\in\mathbb{Z}} p_k \log_2 p_k$ and $D_\epsilon = \sum_{k\in\mathbb{Z}}\int_{t_k}^{t_{k+1}}(y_k - x)^2 f_X(x)dx$, where the reconstruction levels $\{y_k\}$ which minimize distortion for a fixed rate are given by $y_k = \frac{\int_{t_k}^{t_{k+1}} x f_X(x)dx}{p_k}$, as shown in [9].

We consider three cases, namely, $k \le -1$, $k = 0$, $k \ge 1$. From the definitions of p_k and y_k we have, for $k \le -1$

$$\begin{aligned} p_k &= (1-r^2)\frac{e^{-\lambda\Delta(\epsilon+\frac{1}{2})}e^{\lambda k\Delta}(e^{\lambda\Delta}-1)}{2} \\ y_k &= \Delta(k-\frac{1}{2}) - \frac{1}{\lambda} + \Delta\frac{e^{\lambda\Delta}}{e^{\lambda\Delta}-1} \end{aligned} \tag{8}$$

For $k \ge 1$, we have

$$\begin{aligned} p_k &= (1-r^2)\frac{e^{\lambda\Delta(\epsilon+\frac{1}{2})}e^{-\lambda k\Delta}(1-e^{\lambda\Delta})}{2} \\ y_k &= \Delta(k-\frac{1}{2}) + \frac{1}{\lambda} - \Delta\frac{e^{-\lambda\Delta}}{1-e^{-\lambda\Delta}} \end{aligned} \tag{9}$$

For $k = 0$, we have

$$\begin{aligned} p_0 &= r^2 + \frac{(1-r^2)}{2}[2 - e^{-\lambda\Delta(\epsilon+\frac{1}{2})} - e^{\lambda\Delta(\epsilon-\frac{1}{2})}] \\ y_0 &= \frac{\epsilon\Delta}{p_0} + (1-r^2)\frac{e^{-\lambda(\epsilon+\frac{1}{2})\Delta} - (\lambda\Delta+1)e^{\lambda(\epsilon-\frac{1}{2})\Delta}}{2\lambda p_0} \end{aligned} \tag{10}$$

The distortion is given by $D_\epsilon = (1-r^2)\frac{2}{\lambda^2} + \Delta^2\epsilon^2 - \sum_i y_i^2 p_i$. Denoting $\theta \triangleq e^{-\lambda\Delta}$, we compute $A_1 \triangleq \sum_{k\ge 1} y_k^2 p_k$ and $A_3 \triangleq \sum_{k\le -1} y_k^2 p_k$ from (8) and (9)

$$\begin{aligned} A_1 &= (1-r^2)\frac{\theta^{-\epsilon-\frac{1}{2}}}{2\lambda^2}[1 + \frac{\theta\ln^2\theta}{(1-\theta)^2} - \frac{1-\theta(1-\ln\theta)^2}{1-\theta}] \\ A_3 &= (1-r^2)\frac{\theta^{\epsilon+\frac{1}{2}}}{2\lambda^2}[1 + \frac{\theta\ln^2\theta}{(1-\theta)^2}] \end{aligned}$$

From (10), $A_2 \triangleq y_0^2 p_0$ can be computed as

$$A_2 = \frac{[\epsilon\Delta + \frac{(1-r^2)}{2\lambda}(e^{-\lambda(\epsilon+\frac{1}{2})\Delta} - (\lambda\Delta+1)e^{\lambda(\epsilon-\frac{1}{2})\Delta})]^2}{r^2 + \frac{(1-r^2)}{2}[2 - e^{-\lambda\Delta(\epsilon+\frac{1}{2})} - e^{\lambda\Delta(\epsilon-\frac{1}{2})}]}$$

The quantizer distortion is, then, given by

$$D_\epsilon = (1-r^2)\frac{2}{\lambda^2} + \Delta^2\epsilon^2 - A_1 - A_2 - A_3 \tag{11}$$

To compute the quantizer rate, we compute $J_1 \triangleq -\sum_{k\le -1} p_k \log_2 p_k$ and $J_3 \triangleq -\sum_{k\ge 1} p_k \log_2 p_k$

$$\begin{aligned} J_1 &= (1-r^2)[\frac{\theta^{\epsilon+\frac{1}{2}}}{2}(1 + \frac{H(\theta)}{1-\theta} - (\epsilon+\frac{1}{2})\log_2\theta) \\ &\quad - \log_2(1-r^2)\frac{\theta^{\epsilon+\frac{1}{2}}}{2}] \\ J_3 &= (1-r^2)[\frac{\theta^{-\epsilon-\frac{1}{2}}}{2}(1 + \frac{H(\theta)}{1-\theta} + (\epsilon+\frac{1}{2})\theta\log_2\theta \\ &\quad + (1-\theta)(\log_2(1-\theta)-1)) - \log_2(1-r^2)\frac{\theta^{\epsilon-\frac{1}{2}}}{2}] \end{aligned}$$

From (10), $J_2 \triangleq p_0 \log_2 p_0$ can be computed as

$$\begin{aligned} J_2 &= [r^2 + \frac{(1-r^2)}{2}(2 - e^{-\lambda\Delta(\epsilon+\frac{1}{2})} - e^{\lambda\Delta(\epsilon-\frac{1}{2})})] \cdot \\ &\quad \log_2(r^2 + \frac{(1-r^2)}{2}[2 - e^{-\lambda\Delta(\epsilon+\frac{1}{2})} - e^{\lambda\Delta(\epsilon-\frac{1}{2})}]) \end{aligned}$$

The quantizer rate can be computed as

$$R_\epsilon = J_1 + J_2 + J_3 \tag{12}$$

We are now in a position to derive the operational rate-distortion performance for WZ coding, using uniform scalar quantization followed by perfect SW coding, of the desired source. Since the source is memoryless and stationary, we see from (4) that the WZ rate is given by

$$R_{WZ} = H(Q(X)|Y) = \int_{-\infty}^{\infty} H(Q(X)|Y=y)f_Y(y)dy \tag{13}$$

For a fixed value of $Y = y$ the conditional distribution of X is given by $f_{\widehat{Z},\epsilon}(\cdot)$ with $\epsilon = \frac{ry \mod \Delta}{\Delta}$. Further, note that ϵ is distributed as

$$f_\epsilon(\epsilon) = \frac{1}{r}\sum_{k\in\mathbb{Z}} f_Y(\frac{(k+\epsilon)\Delta}{r}) \quad -\frac{1}{2} \le \epsilon \le \frac{1}{2} \tag{14}$$

Thus (13) reduces to

$$R_{WZ} = \sum_{k\in\mathbb{Z}} \int_{-\frac{1}{2}}^{\frac{1}{2}} R_\epsilon f_\epsilon(\epsilon) d\epsilon \tag{15}$$

Similarly the WZ coding distortion can be derived from (5), (14) as

$$D_{WZ} = \sum_{k\in\mathbb{Z}} \int_{-\frac{1}{2}}^{\frac{1}{2}} D_\epsilon f_\epsilon(\epsilon) d\epsilon \tag{16}$$

Equations (15) and (16) can be evaluated numerically to yield the operational rate-distortion function of WZ coding.

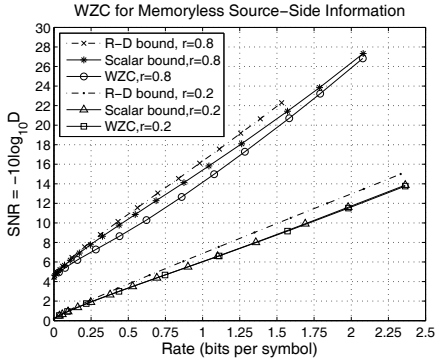

Fig. 2. Comparison of WZ coding to rate-distortion bounds obtained when encoder knows side-information. The figure plots $-10\log_{10} D$ versus R for a unit-variance source with $r = 0.2, 0.8$.

Figure 2 compares the performance of the described WZ coding scheme to the rate-distortion bounds obtained by considering the case where the side-information is known at the encoder, for a unit-variance source with $r = 0.2, 0.8$. The bounds can be evaluated by analyzing the theoretical rate-distortion performance, and the operational rate-distortion performance of mid-tread uniform scalar quantization, for the random variable with density $f_Z(z)$, respectively. In Figure 2, the theoretical rate-distortion curves computed by the Blahut-Arimoto algorithm [10] are shown in the dotted lines. The operational rate-distortion curves can be shown to have the following parametric form, with $0 < \theta < 1$

$$\begin{aligned} R_\theta &= -(1-(1-r^2)\sqrt{\theta})\log_2(1-(1-r^2)\sqrt{\theta}) \\ &\quad +(1-r^2)\sqrt{\theta}[1-\frac{\log_2\theta}{2}-\log_2(1-\theta)-\frac{\theta\log_2\theta}{1-\theta}] \\ &\quad -(1-r^2)\sqrt{\theta}\log_2(1-r^2) \\ D_\theta &= \frac{(1-r^2)}{\lambda^2}[2-\sqrt{\theta}((1-\frac{\ln\theta}{2})^2+\frac{\theta\ln^2\theta}{(1-\theta)^2}] \end{aligned}$$

As shown by the figure the performance loss of WZ coding, compared to the case where the encoder utilizes the side-information during encoding, is very small at very low rates and at high rates. At intermediate rates, there is a non-negligible performance loss for high values of the correlation coefficient r, with a maximum loss of about 1 dB for $r = 0.8$. For $r = 0.2$, on the other hand, the WZ coding performance is nearly coincident with the uniform scalar quantization bound. In the next section we will consider the case where the source has memory, and where the side-information is derived from previously encoded source samples. Our aim will be to characterize the performance loss compared to DPCM coding which utilizes side-information at the encoder.

3. WZ CODING OF LAPLACE-MARKOV SOURCE

We consider the Laplace-Markov source described by (6), and the WZ coding system described by Figure 1. The scalar quantizer used is an asymmetric uniform scalar quantizer with a deadzone, i.e. the partition levels of the quantizer are

$$\begin{aligned} t_k &= \Delta k + \epsilon \qquad k \geq 0 \\ t_k &= \Delta(k+1) - \epsilon \qquad k < 0 \end{aligned}$$

Further, we will set $\epsilon = \Delta$.

For simplicity of illustration we consider the case where the decoder side-information consists of the quantized value of the previous source symbol, i.e. $Q(X_{n-1})$ at time n. It is easy to show that the conditional density

$$f_i(x) = f_{X_n|Q(X_{n-1})=i}(x) = f_{X_n|X_{n-1}\in[t_i,t_{i+1})}(x) \tag{17}$$

is independent of n. Denote the conditional bin probabilities and bin reconstructions as $p_k^i \triangleq \int_{t_k}^{t_{k+1}} f_i(x)dx$ and $y_k^i \triangleq \int_{t_k}^{t_{k+1}} x f_i(x)dx$, respectively. The stationarity of the conditional density in (17) implies that (4) and (5) can be evaluated as

$$\begin{aligned} R_{WZ} &= -\sum_{i\in\mathbb{Z}}(\int_{t_i}^{t_{i+1}} \frac{\lambda}{2}e^{-\lambda|x|}dx)\sum_{k\in\mathbb{Z}} p_k^i \log_2 p_k^i \qquad (18) \\ D_{WZ} &= \sum_{i\in\mathbb{Z}}(\int_{t_i}^{t_{i+1}} \frac{\lambda}{2}e^{-\lambda|x|}dx)\sum_{k\in\mathbb{Z}}\int_{t_k}^{t_{k+1}} f_i(x)(y_k^i - x)^2 dx \end{aligned}$$

The operational rate-distortion function in (18) can be derived by computing $f_i(x)$. From (6), we get that

$$f(x_n|x_{n-1}) = r^2\delta(x_n - rx_{n-1}) + (1-r^2)\frac{\lambda}{2}e^{-\lambda|x_n - rx_{n-1}|}$$

which can be used to evaluate $f_i(x)$ as

$$f_i(x) = \frac{d}{d\alpha}\frac{\int_{-\infty}^{\alpha} dx_k \int_{t_i}^{t_{i+1}} f(x_n|x_{n-1})f_X(x_{n-1})dx_{n-1}}{\int_{t_i}^{t_{i+1}} f_X(x_{n-1})dx_{n-1}} \tag{19}$$

Thus, for example, for $i = -1$ we get the following expression for $f_i(x)$

$$\begin{cases} \frac{\lambda}{4}e^{\lambda\alpha}\frac{-\theta^r(r+1)+2\theta+\theta^{-r}(r-1)}{\theta-1} & \alpha < -r\Delta \\ \frac{\lambda}{4}\frac{\theta^{-r}(r-1)(e^{-\lambda\alpha}+e^{\lambda\alpha})+2\theta e^{\lambda\alpha}}{\theta-1} & \alpha \in [-r\Delta, 0) \\ \frac{\lambda}{4}\frac{\theta^{-r}(r-1)(e^{-\lambda\alpha}+e^{\lambda\alpha})+2\theta e^{-\lambda\alpha}}{\theta-1} & \alpha \in [0, r\Delta) \\ \frac{\lambda}{4}e^{-\lambda\alpha}\frac{-\theta^r(r+1)+2\theta+\theta^{-r}(r-1)}{\theta-1} & \alpha \geq r\Delta \end{cases}$$

where $\theta \triangleq e^{-\lambda\Delta}$.

Equation (19) can be used to derive the operational rate-distortion function by numerical evaluation of (18). For the case where the Laplace-Markov process has low correlation and low-rate, an analytical approximation can be made by discarding quantizer bins far from the mean of the source. The derived rate-distortion function is sufficiently simple to allow presentation here, in (20) and (21)

$$D = \mu_2 - 2A \tag{20}$$

where

$$\mu_2 \triangleq \frac{-2r^2\ln\theta - r^2(\ln\theta)^2 - 2 + 2\theta}{\lambda^2(\theta-1)}$$

$$A \triangleq \frac{1}{4\lambda^2\theta^{r+1}(\theta-1)^3}[(1-\theta)^2(1+2\ln\theta) + (\ln\theta)^2(1-\theta+\theta^2)](r+2\theta^{r+1}-1-(r+1)\theta^{2r})$$

and

$$R = -P\log_2 P + J_1 + J_2 \quad (21)$$

where

$$P \triangleq \frac{1}{2(\theta-1)}[\theta^{r-1}(r+1)+\theta^{-r-1}(1-r)-4+2\theta]$$

$$J_1 \triangleq \frac{-\theta^{-1}}{\theta-1}K_1\log_2 K_1 - \frac{(K_1\log_2 e)(\theta^{-1}-2)}{(\theta-1)^2}\ln\theta$$

$$J_2 \triangleq \frac{-\theta}{\theta-1}K_2\log_2 K_2 + \frac{(K_2\ln\theta)\theta}{(\theta-1)^2}\log_2 e$$

with $K_1 \triangleq -\frac{1}{4}[\theta^r(r+1)-2\theta+(1-r)\theta^{-r}]$ and $K_2 \triangleq \frac{1}{4}[\theta^{-2-r}(r-1)+2\theta^{-1}-(1+r)\theta^{r-2}]$.

4. WZ CODING AND DPCM CODING

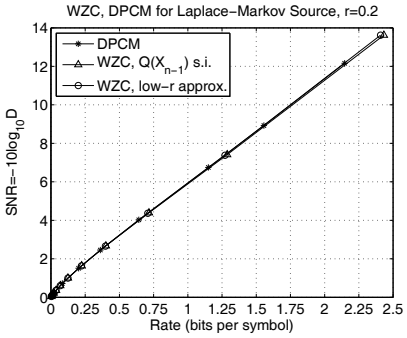

Fig. 3. Comparison of rate-distortion (R-D) curves for uniform scalar quantization and perfect SW coding with DPCM for compression of unit-variance Laplace-Markov source ($r = 0.2$). Plotted are: (1) DPCM R-D curve, (2) WZ coding R-D curve obtained by simulation, and (3) Low-correlation R-D curve derived in Section 3. The three curves are nearly coincident.

We consider a unit-variance Laplace-Markov source with $r = 0.2$ (low correlation) and $r = 0.8$ (high correlation). In this section we compare the operational rate-distortion performance of WZ coding with that of DPCM coding with the aim of characterizing the performance gap. The DPCM coder uses $\rho\hat{X}_{n-1}$ to approximate $E[\cdot]$ in (1). Simulations of WZ coding and DPCM are performed by encoding blocks of $10^5 - 10^6$ source vectors simulated over 50 time-steps.

Figure 3 compares the simulated operational performance of WZ coding with that of DPCM coding for $r = 0.2$. The WZ decoder uses $Q(\widehat{X}_{n-1})$ as side-information at time-step n. Also shown is the low-correlation rate-distortion function given by (20) and (21). As the figure shows, the derived rate-distortion function is a very good fit for the operational rate-distortion function obtained through simulation upto $R = 2.5$ bits. Further, the figure shows that there is a negligible performance gap between WZ coding and DPCM in this case, similar to the memoryless case.

Figure 4 compares the simulated operational performance of WZ coding with that of DPCM coding for the high correlation case where $r = 0.8$. There are two WZ coders considered; the first uses $Q(\widehat{X}_{n-1})$ as decoder side-information, while the second improves upon this by using $\widehat{X}_{n-1}$ as decoder side-information. As the figure shows, there

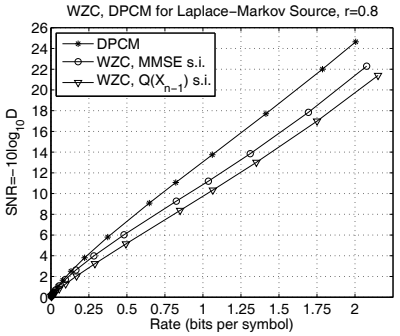

Fig. 4. Comparison of rate-distortion (R-D) curves for uniform scalar quantization and perfect SW coding with DPCM for compression of unit-variance Laplace-Markov source ($r = 0.8$). Plotted are: (1) DPCM R-D curve, (2) WZ coding R-D curve with MMSE side-information $\widehat{X}_{n-1}$, and (3) WZ coding R-D curve with side-information $Q(X_{n-1})$.

is a significant gap between DPCM coding and WZ coding at intermediate rates. As expected, the coder which uses $\widehat{X}_{n-1}$ performs better than the other WZ coder, but it nevertheless loses upto 2 dB compared to DPCM at rates around 1-2 bits per symbol. This indicates that WZ coding may require a larger decoder history for efficiently compressing low-innovation Laplace-Markov sources at such rates, than just the previous symbol, unlike typical current practice.

5. REFERENCES

[1] A.D. Wyner and J. Ziv, "The rate-distortion function for source coding with side information at the decoder," *IEEE Trans. Inform. Theory*, vol. 22, pp. 1–10, Jan. 1976.

[2] D. Slepian and J. Wolf, "Noiseless coding of correlated information sources," *IEEE Trans. Inform. Theory*, vol. 19, pp. 471–480, July 1973.

[3] V. Stankovic, A.D. Liveris, Z. Xiong, and C.N. Georghiades, "On code design for the slepian-wolf problem and lossless multiterminal networs," *IEEE Trans. Image Proc.*, vol. 52, pp. 1495–1507, Apr. 2006.

[4] B. Girod, A. Aaron, S. Rane, and D. Rebollo-Monedero, "Distributed video coding," *Proc. IEEE*, vol. 93, pp. 71–83, Jan. 2005.

[5] V. Sheinin, A. Jagmohan, and D. He, "Uniform threshold scalar quantizer performance in wyner-ziv coding with memoryless, additive laplacian correlation channel," in *Proc. IEEE Conf. Acoust. Speech Sig. Proc.*, May 2006, pp. 217–221.

[6] R.C. Reininger and J.D. Gibson, "Distributions of the two-dimensional dct coefficients for images," *IEEE Trans. Comm.*, vol. 31, pp. 835–839, June 1983.

[7] K. Rose and S.L. Regunathan, "Toward optimality in scalable predictive coding," *IEEE Trans. Image Proc.*, vol. 10, pp. 965–976, July 2001.

[8] N. Farvardin and J. Modestino, "Rate-distortion performance of dpcm schemes for autoregressive sources," *IEEE Trans. Inform. Theory*, vol. 31, pp. 402–418, May 1985.

[9] T. Berger, "Optimum quantizers and permutation codes," *IEEE Trans. Inform. Theory*, vol. 18, pp. 759–765, Nov. 1972.

[10] T. Cover and J. Thomas, *Elements of Information Theory*, Wiley, 1991.